

THE ELECTROCHEMICAL OXIDATION OF VARIOUS SUBSTITUTED MANDELIC
ACIDS: AN ELECTROCHEMICAL AND PRODUCT ANALYSIS STUDY

by

MAURICE ROGER CLAEYS

B.A., Coe College, 1987

A THESIS

submitted in partial fulfillment of the
requirements for the degree

MASTER OF SCIENCE

CHEMISTRY

KANSAS STATE UNIVERSITY

Manhattan, Kansas

1989

Approved by:

M. Dale Hawley
M. Dale Hawley

Table of Contents

Acknowledgement	1
Introduction	2
Results and Discussion	4
Cyclic Voltammetry Data for 3,4-Dihydroxymandelic Acid	4
Cyclic Voltammetry Data for 3,4-Dihydroxybenzaldehyde	6
Coulometric Data for 3,4-Dihydroxymandelic Acid	8
Coulometric Data for 3,4-Dihydroxybenzaldehyde	9
SPSCA Data for 3,4-Dihydroxymandelic Acid	10
Analysis of Mono-Phenol Analogues of 3,4-Dihydroxymandelic Acid	13
Cyclic Voltammetric Data for 4-Hydroxymandelic Acid and 3-Hydroxymandelic Acid	14
SPSCA Data for 4-Hydroxymandelic acid and 4-hydroxybenzaldehyde	14
3-Hydroxymandelic Acid and 3-Hydroxybenzaldehyde	15
3-Methoxy-4-Hydroxymandelic Acid and 4-Methoxy-3-Hydroxymandelic Acid	16
Cyclic Voltammetric Data for 3-Methoxy-4-Hydroxymandelic Acid and 4-Methoxy-3-Hydroxymandelic Acid	17
Product Analysis for 3-Methoxy-4-Hydroxymandelic Acid and 4-Methoxy-3-Hydroxymandelic Acid	17
SPSCA Data for 3-Methoxy-4-Hydroxymandelic Acid and 4-Methoxy-3- Hydroxymandelic Acid	19
Concluding Remarks	20
Experimental Section	22
Solution Conditions	22
Electrochemical Instrumentation	23

LD
3668
.74
CHEM
1989
C53
A. Z

Electrochemical Procedures	23
HPLC Analysis of Oxidation Products	24
References	26

Figures and Tables

Table 1:

Cyclic voltammetric and chronoamperometric data on the oxidation of disubstituted mandelic acids. 28

Table 2:

Rate constants (k) for the oxidative decarboxylation of 3,4-dihydroxymandelic acid at several values of pH. 29

Table 3:

Analysis of the products formed upon the coulometric oxidation of methoxy derivatives of 3,4-dihydroxymandelic acid at different potentials after $2 e^-$ /molecule. 30

Figure 1:

Proposed oxidative metabolites of N-acyl catecholamines involved in sclerotization of insect cuticle. 31

Figure 2:

Proposed cross-links between N-acyl catecholamines and proteins. 32

Figure 3:

Cyclic voltammogram of 3,4-dihydroxymandelic acid at pH 2 and a scan rate of 0.2 V/s. 33

Figure 4:

Cyclic voltammogram for 2.04 mM 3,4-dihydroxybenzaldehyde at pH 2 and a scan rate of 0.066 V/s. 34

Figure 5:

Cyclic voltammogram for 2.04 mM 3,4-dihydroxybenzaldehyde at pH 2 and a scan rate of 0.2 V/s. 35

Figure 6:

Cyclic voltammogram for 2.04 mM 3,4-dihydroxybenzaldehyde
at pH 2 and a scan rate of 0.66 V/s. 36

Figure 7:

Product studies after the controlled-potential coulometric
oxidation of 3,4-dihydroxymandelic acid at pH 6 as a
function of n value. 37

Figure 8:

Product studies after the controlled-potential coulometric
oxidation of 3,4-dihydroxymandelic acid at pH 2 as a
function of n value. 38

Figure 9:

Standard curves for various equilibrium constants for an
ECE mechanism. 39

Figure 10:

Kinetics plot of SPSCA results for the oxidative
decarboxylation of 3,4-dihydroxymandelic acid at pH 6. 40

Figure 11:

Product studies after the controlled-potential coulometric
oxidation of 4-hydroxymandelic acid at pH 6 as a function
of n value. 41

Figure 12:

Proposed mechanism for the oxidation of 3,4-dihydroxymandelic
acid. 42

Acknowledgments

This work was done as a collaborative study on the oxidative mechanism of various compounds structurally related to phenolic substances involved in the sclerotization of insect cuticle. Personnel in the Departments of Chemistry and Entomology at Kansas State University, along with the USDA Grain Marketing Research Laboratory, Manhattan, Kansas, were involved with different aspects of this project. For additional insect related data, the reader may refer to the Ph.D. Dissertation of Thomas Czaplá, Department of Entomology, Kansas State University, 1989. This work was supported in part by grants (CHE-86-14657, DCB-86-09717) from the National Science Foundation.

Introduction

The sclerotization or hardening of insect cuticle, a composite material composed of protein, chitin, lipid, and other components, involves the oxidation of different catecholamines to quinone-type intermediates which then form cross-links with cuticular neuromolecules. There are three oxidative metabolites of N-acyl catecholamines that have been proposed to act as non-linking agents in the process of sclerotization. The first mechanism is called quinone tanning sclerotization and involves the substrate being oxidized to an *o*-quinone¹. The second mechanism, β -sclerotization, involves the formation of a quinone methide², while the third, α,β sclerotization, involves the formation of a double bond between the α,β carbons of the side-chain on the diphenolic ring (Fig. 1)³. Each of these mechanisms leads to a unique cross-link between the N-acyl catecholamine and cuticular protein or chitin (Fig. 2)⁴⁻⁹. The actual mechanistic pathway of the sclerotization of the insect cuticle is unknown, but is being quite actively investigated at the present time.

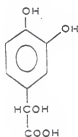
One of the model compounds that can be used for study of cuticular oxidative reactions is 3,4-dihydroxymandelic acid (1). The enzymatic oxidation of 3,4-dihydroxymandelic acid by mushroom tyrosinase yielded 3,4-dihydroxybenzaldehyde (2) as a major product, and it was speculated that 3,4-dihydroxymandelic acid was oxidized directly to the *p*-quinone methide intermediate rather than to the corresponding *o*-quinone¹⁰. However, other investigators have provided evidence that the oxidation initially leads to formation of the traditional *o*-quinone and that this species then undergoes either a charge-transfer complex reaction with

starting material or chemical decarboxylation^{11,12} to form a quinone methide. Quinone methides have been proposed as reactive intermediates in many different types of biological processes, such as the sclerotization of insect cuticle¹³, the biosynthesis of biopolymer lignins¹⁴, and the mediation of adrenergic responses to catecholamines¹⁵.

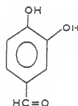
It was the goal of this research to determine the structure of the intermediates produced during the electrochemical oxidation of 3,4-dihydroxymandelic acid and to establish the chemical mechanism involved in the production of 3,4-dihydroxybenzaldehyde. 3,4-Dihydroxymandelic acid, besides being involved in the sclerotization of cuticle in some insect species, is found as a product in the mitochondrial oxidation of norepinephrine, a neurotransmitter in biological systems. The advantage of electrochemical oxidations over enzymatic oxidations for mechanistic determinations is the fact that electrochemical methods allow the observation of reaction intermediates that do not have long enough lifetimes to be observed by normal detection methods (UV absorbance) used to follow enzymatic oxidations.

Previous studies have shown that the product distribution from an electrochemical oxidation or reduction may be altered by a change of electrode potential¹⁶. If the product distribution can be affected significantly by altering the electrode potential in this reaction, this behavior might explain why several different mechanistic pathways have been proposed for this reaction. To determine if one or more reaction pathways are possible, we determined the products formed as a function of electrode potential. Various substituted mandelic acids were also

studied in an attempt to elucidate the mechanism for the oxidation of 3,4-dihydroxymandelic acid.



1



2

3,4-Dihydroxymandelic Acid

3,4-dihydroxybenzaldehyde

Results and Discussion

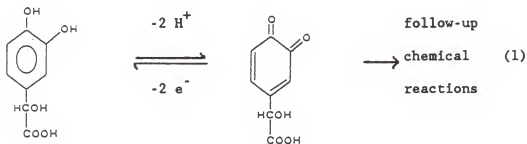
Cyclic Voltammetric Data for 3,4-Dihydroxymandelic Acid.

Cyclic voltammetry (CV) is probably the most useful electrochemical technique for quickly diagnosing an electrode reaction. In CV, the electrode potential is varied linearly over a potential range to determine the oxidation-reduction potential of each electroactive species that is either present initially in solution or produced as an electrode product. The oxidation-reduction potential of the electroactive species is characteristic of a given compound, thus assisting in the identification of the electroactive species. In our experiments, the scan is initiated in the positive-going direction. When the potential becomes sufficiently positive, it will oxidize the compound at the electrode surface. After oxidation of the compound in question, the scan direction can be reversed in order to ascertain the fate of the electrode product. If the system is chemically reversible, the potential will eventually become sufficiently negative such that the

electrogenerated oxidation product is reduced to starting material. The oxidation and reduction peaks should have the same peak height if the system is electrochemically reversible. If the initial oxidation product is consumed by a subsequent chemical reaction, the reduction peak will be reduced by an amount proportional to the quantity of electrogenerated material consumed by the chemical reaction.

Cyclic voltammograms of the mandelic acid series displayed anodic peaks ranging from 0.77 V for 3-methoxy-4-hydroxymandelic acid to 0.95 V for 4-hydroxymandelic acid at pH 6 ($\nu = 0.2$ V/s), whereas the corresponding benzaldehydes oxidized at less positive potentials at the same pH (Table 1). Cyclic voltammograms of 3,4-dihydroxymandelic acid displayed a chemically reversible couple with its corresponding o -quinone at $\nu \geq 5$ V/s ($E_{p(a)} = 0.85$ V, $E_{p(c)} = -0.25$ V). The peak separation ($E_{p(a)} - E_{p(c)}$) of 1.1 V at $\nu = 5$ V/s greatly exceeds that of 30 mV for an electrochemically reversible two-electron process. The reason for the larger than normal peak separation for this reversible couple is a slow heterogeneous electron transfer rate (rate of electron transfer from the electrode surface to the substrate). As the scan rate was decreased from 20 V/s to 1 V/s, the relative peak height for the reduction of the 3,4-dihydroxymandelic acid o -quinone at -0.25 V decreased. Concomitantly, a new cathodic peak arose at 0.1 V and grew at the expense of the cathodic peak for the reduction of the 3,4-dihydroxymandelic acid o -quinone. At slower scan rates ($\nu \leq 2$ V/s), the anodic peak shifted from 0.78 V on the first scan to 0.55 V on subsequent scans, which corresponds to a new electroactive species (EAS) in solution being formed (equation 1). When the scan rate was decreased

to under 1 V/s, the cathodic peak at 0.1 V decreased in relative peak height as a third cathodic peak at 0.0 V increased in relative peak height (Fig. 3). Cyclic voltammograms of 3,4-dihydroxymandelic acid at a scan rate of 0.2 V/s (pH 6,) displayed a major anodic peak at 0.78 V and a small cathodic peaks at 0.0 V and 0.1 V on the initial scan. On subsequent scans, the anodic peak at 0.78 V shifted to 0.55 V.

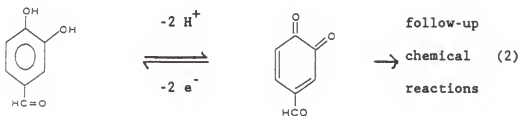


3,4-Dihydroxymandelic Acid Corresponding *o*-quinone

Cyclic Voltammetric Data for 3,4-Dihydroxybenzaldehyde.

3,4-Dihydroxybenzaldehyde afforded cyclic voltammetric behavior consisting of an anodic peak at 0.55 V and a cathodic peak at 0.1 V (pH 6, $\nu > 5$ V/s). The cathodic peak at 0.1 V, which represents the reduction of the corresponding *o*-quinone back to 3,4-dihydroxybenzaldehyde (Figs. 4-6), decreased in relative peak height as the scan rate was decreased from 5 V/s to 0.2 V/s. Concomitantly, a cathodic peak appeared at 0.0 V and grew in relative magnitude as the cathodic peak at 0.1 V decreased. The EAS that is reduced at 0.0 V is produced from a follow-up chemical reaction involving the 4-formyl-*o*-benzoquinone

(equation 2). Anodic peak potentials were shifted in the positive direction at lower pH in both the mandelic acid (shifted about 0.1 V, $\gamma = 0.2$ v/s, as the pH was decreased from 6 to 2) and benzaldehyde series (shifted about 0.2 V, $\gamma = 0.2$ v/s, as the pH was decreased from 6 to 2). Lower pH value (pH < 2) cyclic voltammograms of 3,4-dihydroxybenzaldehyde displayed a larger cathodic peak for the reduction of 4-formyl-*q*-benzoquinone as compared to the corresponding peak height at pH 6 ($\gamma = 0.2$ V/s). This would suggest that the 4-formyl-*q*-benzoquinone is more stable at pH 2 than at pH 6. 3,4-Dihydroxybenzaldehyde was identified in the 3,4-dihydroxymandelic acid cyclic voltammograms by a shift in the anodic peak from 0.78 V to 0.55 V on the second positive-going scan. The 3,4-dihydroxybenzaldehyde formed during the first scan is oxidized on the second positive-going scan, thus producing a shift in the anodic peak potential. Product analysis by HPLC and GC-MS also showed the formation of 3,4-dihydroxybenzaldehyde in the controlled-potential, coulometric oxidation of 3,4-dihydroxymandelic acid.



3,4-Dihydroxybenzaldehyde

4-Formyl-*q*-benzoquinone

Coulometric Data for the Oxidation of 3,4-Dihydroxymandelic Acid.

Coulometry is an electrochemical technique used to electrolyze large quantities of substrate for product analysis. In coulometric experiments a large electrode and stirring of the solution are employed to oxidize the substrate completely in a reasonably short period of time. Coulometric oxidations of 3,4-dihydroxymandelic acid revealed that the total n value (the number of electrons removed per molecule) upon complete oxidation was six, which was greater than the expected four (assuming the product is 4-formyl-*o*-benzoquinone). Buffer components were not oxidized at the various oxidation potentials used in the coulometric experiments ($n \leq 0.25$ for all potentials). Product analysis by HPLC at $n = 2$ (pH 6) indicated complete oxidation of 3,4-dihydroxymandelic acid and a maximum yield of 3,4-dihydroxybenzaldehyde of 60%, based on the amount of starting material consumed (Fig. 7). Product analysis at pH = 2 ($n = 2$) displayed approximately equal quantities of 3,4-dihydroxymandelic acid (45% of starting material remaining) and 3,4-dihydroxybenzaldehyde (78% yield, based on the amount of starting material oxidized) in solution (Fig. 8). Other UV-absorbing, unknown products were formed on continued electrolysis. The coulometric results indicate that at pH 6, the 4-formyl-*o*-benzoquinone oxidizes 3,4-dihydroxymandelic acid, but at pH 2 this electron transfer does not occur. A speculative explanation for this observation is that the follow-up chemical reaction involving 4-formyl-*o*-benzoquinone going on to other reaction products is pH dependent and has an effect on the reaction mechanism.

No change in product distribution was observed when 3,4-dihydroxy-mandelic acid was oxidized at different potentials. The products observed following coulometric oxidation of 3,4-dihydroxymandelic acid were similar to the products formed upon complete oxidation of 3,4-dihydroxybenzaldehyde. This result supports the hypothesis that 3,4-dihydroxybenzaldehyde, which is formed in the oxidation of 3,4-dihydroxymandelic acid, is also being oxidized at this potential ($E = 1.2$ V). As shown by CV, 3,4-dihydroxybenzaldehyde is more readily oxidized than the 3,4-dihydroxymandelic acid in the pH range from 2 to 6.

Coulometric Data for 3,4-Dihydroxybenzaldehyde.

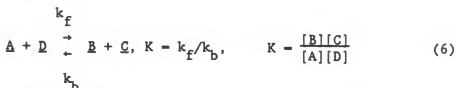
The exhaustive, coulometric oxidation of 3,4-dihydroxybenzaldehyde, which occurs more readily than the oxidation of 3,4-dihydroxymandelic acid, was found to be an overall four-electron process. Product analysis following complete oxidation of 3,4-dihydroxybenzaldehyde yielded multiple UV-absorbing products at low yields which have not been identified. Accordingly, because of the oxidation of 3,4-dihydroxybenzaldehyde to 4-formyl-*o*-benzoquinone is a two-electron process, the two additional electrons per molecule in the coulometric oxidation of 3,4-dihydroxymandelic acid must be accounted for by the oxidation of electroactive products arising from the decomposition of 4-formyl-*o*-benzoquinone. These other EAS may form dimeric and/or polymeric compounds similar to the dimeric products shown to form in various other substituted catechol systems¹⁷.

SPSCA Results for 3,4-Dihydroxymandelic Acid.

The electrochemical technique used to determine rate constants in reaction mechanisms in this research was single-potential-step chronoamperometry (SPSCA). SPSCA is performed by setting the initial electrode potential such that no species in solution is either oxidized or reduced. The electrode potential is then stepped sufficiently positive such that the concentration of the EAS at the electrode surface is zero. The rate of reduction of the EAS at this potential is limited by the diffusion rate of the EAS to the electrode from bulk solution. The relationship between the current and time for a diffusion-controlled process is given by the Cottrell equation: $it^{1/2} = \frac{nFAD^{1/2}C^b}{\pi^{1/2}}$, where i = current, t = time, n = number of electrons involved in the reaction, F = Faraday's constant, A = area of the electrode surface, D = diffusion coefficient, C^b = concentration of species in the bulk solution. If $it^{1/2}$ is equal to a constant, the reaction is diffusion controlled and $it^{1/2}$ is directly proportional to the number of electrons involved in the reaction.

If there is a homogeneous chemical reaction occurring to give an additional EAS, then the n value may be kinetically controlled. SPSCA results were plotted as $it^{1/2}/C$ (concentration) vs. $\log t$. Chronoamperometric n values were calculated assuming that the oxidation of 1,2-dihydroxybenzene is a diffusion-controlled two-electron process and that the diffusion coefficients of 1,2-dihydroxybenzene and 3,4-dihydroxymandelic acid are similar. The chronoamperometric oxidation of 3,4-dihydroxymandelic acid afforded n_{app} vs. $\log t$ behavior

consistent with an ECE mechanism (a first-order homogeneous Chemical reaction interposed between two Electron-transfer processes; equations 3-6). The chronoamperometric (CA) data for 3,4-dihydroxybenzaldehyde, plotted as $it^{1/2}$ versus $\log t$, yielded a diffusion-controlled two-electron process for times under ten seconds. In the ECE mechanistic scheme, A is the starting material, 3,4-dihydroxymandelic acid; B is the initial two-electron oxidation of A; C is 3,4-dihydroxybenzaldehyde; and D is the two-electron oxidation product of C, 4-formyl-Q-benzoquinone. The rate-determining step is presumed to be the loss of CO_2 from the oxidized intermediate B. The first-order rate constant was determined by plotting n_{app} vs. $\log t$ and comparing these plots to digitally simulated curves for an ECE process. The theoretical curves were obtained from digital simulations of a standard ECE reaction as described by equations 3 - 6 and $K = 0/0$ (Fig. 9):

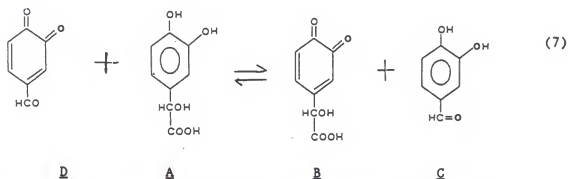


$K = 0/0$ defines a reaction in which both k_f and k_b equal to zero, i.e., the homogeneous electron transfer reaction (equation 6) does not occur. The rate constant, which increased monotonically by a factor of approximately 14 as the pH was increased from 1 to 8, was determined to be $k = 1.58 \text{ s}^{-1}$ at pH 6 (Fig. 10). Because the observed rate constant was independent of the concentration of 3,4-dihydroxymandelic acid

between 0.5 mM to 4.0 mM, we conclude that the chemical reaction occurring subsequent to the oxidation of 3,4-dihydroxymandelic acid is first-order with respect to the starting substrate at these concentrations. Lower pH values (pH 6 to pH 1) afforded rate constants of slightly lower values (Table 2), but this change in rate constant is smaller than expected for a reaction where a proton is involved in the rate-determining step. Since the expected pK_a for 3,4-dihydroxymandelic acid is 3.75 to 4.0, we would normally expect a change in the rate constant in the explored pH range in which $\log k$ increases linearly with pH for $pH < pK_a$. Since we observe no such change in the rate constant in this pH range, the acidity of 3,4-dihydroxymandelic acid o -quinone may be much greater than that of 3,4-dihydroxymandelic acid.

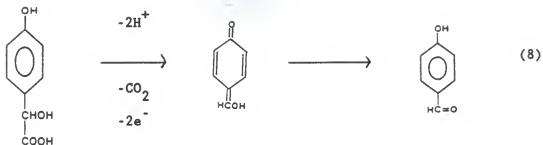
A change in the shape of the kinetic curve from $K = 0/0$ to $K > 1$ was observed as the pH was decreased from 6 to 1. This change in the equilibrium constant is caused by the effect of reaction 6 coming into effect in the reaction mechanism. From the cyclic voltammetric data for 3,4-dihydroxymandelic acid and 3,4-dihydroxybenzaldehyde, we find that 3,4-dihydroxymandelic acid, which has a hydroxyl group on the carbon alpha to the ring, is oxidized at a more positive potential than 3,4-dihydroxybenzaldehyde. On the basis of this result, an equilibrium constant that is less than one might be predicted at pH 6. This would mean that 4-formyl- o -benzoquinone (D) should not oxidize the 3,4-dihydroxymandelic acid (A). Intuitively, however, we would expect an alcohol to be oxidized at a less positive potential than an aldehyde. The SPSCA results are consistent with what we intuitively expect for this type of system. The reason for this inconsistency in the CV and

SPSCA data are the slow rates for the electrochemical oxidation of 3,4-dihydroxymandelic acid (equations 3 and 5) and the chemical oxidation of 3,4-dihydroxymandelic acid by 4-formyl-*p*-benzoquinone (equation 7) at pH 6. As shown above, slow heterogeneous electron transfer at a carbon paste electrode is evidenced in the cyclic voltammogram of 3,4-dihydroxymandelic acid by a much larger separation in peak potentials ($E_{p(a)} - E_{p(c)} > 1 \text{ V}$) than expected for an electrochemically reversible couple ($E_{p(a)} - E_{p(c)} = 30 \text{ mV}$).



Electrochemical Studies of Mono-Phenol Analogues of 3,4-Dihydroxymandelic Acid.

Electrochemical studies of mono-phenol analogues of 3,4-dihydroxymandelic acid were conducted to elucidate the oxidative decarboxylation mechanism. 4-Hydroxymandelic acid and 3-hydroxymandelic acids were used with the hypothesis that the 4-hydroxymandelic acid might undergo a two-electron oxidation to form a *p*-quinone methide, which might then isomerize to give 4-hydroxybenzaldehyde (equation 8), while 3-hydroxymandelic acid would not.



4-Hydroxymandelic Acid para Quinone Methide 4-Hydroxybenzaldehyde

Cyclic Voltammetric Data for 4-Hydroxymandelic Acid and 3-Hydroxymandelic Acid.

Cyclic voltammograms of 4-hydroxymandelic acid displayed an oxidation peak at 0.95 V with no reductive peaks in the potential range of our experimental conditions. Electrode fouling was evident when multiple scans were attempted using the same electrode surface. The cyclic voltammetric anodic peak height for the oxidation of 4-hydroxymandelic acid decreased by about 50% with each successive scan with the same electrode surface. Fouling may be caused by deposition on the electrode surface of polymeric or insoluble materials. The 3-hydroxymandelic acid cyclic voltammogram showed an anodic peak at 0.9 V and a very broad cathodic peak at about -0.1 V on the first cycle. On subsequent cycles, the anodic peak shifted from 0.9 V to about 0.6 V, which indicates that a new EAS has been formed.

SPSCA Data for 4-Hydroxymandelic Acid and 4-Hydroxybenzaldehyde.

SPSCA data for both 4-hydroxymandelic acid and 4-hydroxybenzaldehyde were consistent with an initial two-electron process that afforded products which immediately (<1 sec) fouled the electrode surface. A kinetics study of the oxidation of 4-hydroxymandelic acid was not possible because of the fouling. Fouling of the electrode

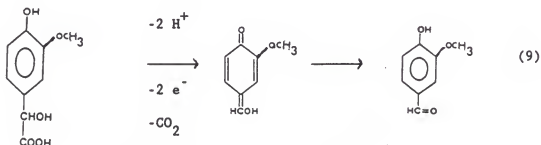
surface was manifested by the reduction in the n value from 2 to less than 0.3, in under one second, in the SPSCA experiments. Despite electrode fouling, coulometric oxidation of 4-hydroxymandelic acid was attempted using a reticulated vitreous carbon electrode. The time required for oxidation of 4-hydroxymandelic acid on a fouled electrode was about three times longer than the time required for oxidation of 3,4-dihydroxymandelic acid on a non-fouled electrode. Product analysis as a function of n value during the coulometric oxidation of 4-hydroxymandelic acid revealed the production of 4-hydroxybenzaldehyde as the major product (95% yield based on the amount of starting material oxidized) and minor quantities (< 5%) of 3,4-dihydroxybenzaldehyde ($n = 3$, Fig. 11). Product analysis revealed a nearly quantitative yield of 4-hydroxybenzaldehyde from 4-hydroxymandelic acid.

3-Hydroxymandelic Acid and 3-Hydroxybenzaldehyde.

SPSCA data for 3-hydroxymandelic acid displayed a straight two-electron process that did not foul the electrode surface or exhibit a kinetically controlled region as was found for 3,4-dihydroxymandelic acid. Analysis of the oxidation products of 3-hydroxymandelic acid showed formation of small amounts of 3-hydroxybenzaldehyde (less than 2% yield, based upon the amount of starting material oxidized) and 3,4-dihydroxybenzaldehyde (less than 1% yield). A large amount of an unknown product was also present (~36% yield of starting material oxidized, assuming an UV absorbance similar to that of 3,4-dihydroxybenzaldehyde).

3-Methoxy-4-Hydroxymandelic Acid and 3-Hydroxy-4-Methoxymandelic Acid.

3-Methoxy-4-hydroxymandelic acid and 3-hydroxy-4-methoxymandelic acid were examined electrochemically to help elucidate the actual mechanism of the oxidation of 3,4-dihydroxymandelic acid. The oxidation of 3-methoxy-4-hydroxymandelic acid was predicted to yield only 3-methoxy-4-hydroxybenzaldehyde if the quinone methide is the initial oxidation product.



3-Methoxy- 4-Hydroxymandelic Acid	Quinone Methide	3-Methoxy- 4-Hydroxybenzaldehyde
--------------------------------------	--------------------	-------------------------------------

On the other hand, the position of the methoxy group in 3-hydroxy-4-methoxymandelic acid presumably prevents oxidation directly to a quinone methide intermediate. If 3,4-dihydroxybenzaldehyde is produced during the oxidation of 3-hydroxy-4-methoxymandelic acid, an *o*-quinone intermediate is presumed to have been formed as an intermediate. Earlier work has shown that loss of methanol from 2- and 4-methoxyphenol is rapid when these compounds are oxidized to give their corresponding benzoquinones¹⁸.

Cyclic Voltammetric Data for 3-Methoxy-4-Hydroxymandelic Acid and 3-Hydroxy-4-Methoxymandelic Acid.

Cyclic voltammograms of 3-methoxy-4-hydroxymandelic acid displayed an oxidation peak at 0.77 V with no cathodic peak discernible, which means that the oxidized form of 3-methoxy-4-hydroxymandelic acid forms a non-EAS in solution. Fouling of the electrode surface was evident with multiple scans on the same electrode surface without a shift in the position of the anodic peak. Cyclic voltammograms of 3-hydroxy-4-methoxymandelic acid displayed an oxidation peak at 0.80 V and small cathodic peaks at 0.15 and 0.05 V. The cathodic peak potentials in the cyclic voltammogram of 3-hydroxy-4-methoxymandelic acid are similar to those of 3,4-dihydroxybenzaldehyde (peaks at 0.10 V and 0.01 V). Multiple scans of 3-hydroxy-4-methoxymandelic acid yielded an anodic peak at 0.50 V, similar to that for the anodic peak of 3,4-dihydroxybenzaldehyde at 0.55 V. The variation in the peak potentials between these different CV may be due to variations in the electrode surface. The cyclic voltammograms of 3-hydroxy-4-methoxymandelic acid suggest that 3,4-dihydroxybenzaldehyde may be involved in the oxidative mechanism of this compound.

Analysis of the Oxidation Products of 3-Methoxy-4-Hydroxymandelic Acid and 3-Hydroxy-4-Methoxymandelic Acid.

Coulometric oxidation products of 3-methoxy-4-hydroxymandelic acid and 3-hydroxy-4-methoxymandelic acid varied depending upon the oxidation potential. Oxidation of 3-methoxy-4-hydroxymandelic acid at 0.8 V yielded 3-methoxy-4-hydroxybenzaldehyde (14% yield, based on the amount of the starting material that was oxidized) at concentrations 70 times

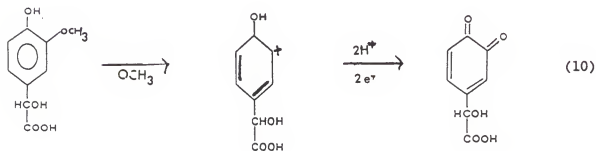
greater than that of 3,4-dihydroxybenzaldehyde (0.2% yield) (Table 3). Oxidation at 1.2 V, however, produced 3-methoxy-4-hydroxybenzaldehyde (2% yield) and 3,4-dihydroxybenzaldehyde (2% yield, based on the amount of starting material that was oxidized) in equal amounts. About 43% of the starting material in the 0.8 V oxidation and 28% of the starting material in the 1.2 V oxidation are unaccounted for in this product analysis at $n = 2$. A change in product distribution was also observed during the oxidation of 3-hydroxy-4-methoxymandelic acid at 0.6 and 1.2 V. Both 3-hydroxy-4-methoxybenzaldehyde (4% yield, based on the amount of starting material that was oxidized) and 3,4-dihydroxybenzaldehyde (4% yield) were produced in equal concentrations at 0.6 V, whereas 3,4-dihydroxybenzaldehyde (19% yield, based on the amount of starting material that was oxidized) was produced at concentrations 95 times greater than that of 3-hydroxy-4-methoxybenzaldehyde (0.2% yield) at 1.2 V (Table 3).

The change in product distribution with a change in oxidation potential may indicate that more than one mechanism is possible in the oxidation of these compounds. Using a severely fouled electrode produced considerably different product yields, where a severely fouled electrode is defined as an electrode that requires a considerably longer time (two to four times as long) to oxidize a given amount of substrate as compared to the time required to oxidize the same amount of substrate with a non-fouled electrode. Oxidation of 3-methoxy-4-hydroxymandelic acid with a fouled electrode produced a greater yield of 3-methoxy-4-hydroxybenzaldehyde (57% yield, based on the amount of starting material that was oxidized) from the starting material and a drastic change in

the amount of starting material remaining (29% of starting amount, Table 3).

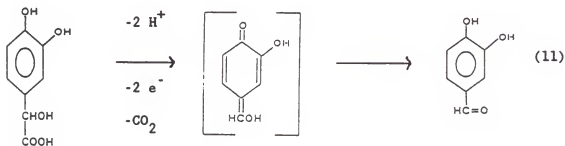
SPSCA Data for 3-Methoxy-4-Hydroxymandelic Acid and 3-Hydroxy-4-Methoxymandelic Acid.

SPSCA ($E_{\text{applied}} > 1.2 \text{ V}$) of both 3-methoxy-4-hydroxymandelic acid and 3-methoxy-4-hydroxybenzaldehyde were two-electron processes initially, which fouled the electrode surface in under one second. The SPSCA ($E_{\text{applied}} = 1.2 \text{ V}$) of 3-hydroxy-4-methoxymandelic acid, however, afforded behavior consistent with that for an ECE mechanism with rate constants indistinguishable from the rate constant for the oxidative decarboxylation of 3,4-dihydroxy mandelic acid. This is consistent with rapid transformation of the initial carbonium ion into the corresponding o -quinone, followed by the rate determining loss of CO_2 from the o -quinone (equation 10).



Concluding Remarks.

Several plausible mechanisms for the formation of 3,4-dihydroxybenzaldehyde upon oxidation of 3,4-dihydroxymandelic acid have been presented in the literature. One involves the initial production of the corresponding *o*-quinone that can undergo either rate-determining decarboxylation to a give quinone methide intermediate or rate-determining tautomerization to a quinone methide that then rapidly decarboxylates^{19,20}. A second mechanism that has been proposed in the literature is a mechanism involving an immediate decarboxylation of the 3,4-dihydroxymandelic acid forming directly a quinone methide which rearranges to form 3,4-dihydroxybenzaldehyde²¹ (equation 11).



3,4-Dihydroxy-
Mandelic Acid

Quinone Methide
Intermediate

3,4-Dihydroxy-
Benzaldehyde

All of the substrates, 4-hydroxymandelic acid, 4-hydroxybenzaldehyde, 3-methoxy-4-hydroxymandelic acid, and 3-methoxy-4-hydroxybenzaldehyde, that we proposed would oxidize by a direct quinone methide mechanism fouled the electrode surface. The fouling of the electrode surface with these substrates indicates that they oxidize by a

different mechanism than 3,4-dihydroxymandelic acid. The mechanistic pathway that this group of compounds oxidize by is unclear at the present time. The indistinguishable rate constants of 3,4-dihydroxymandelic acid and 3-hydroxy-4-methoxymandelic acid suggests that these two compounds form intermediates which undergo the same rate determining step.

The enzymatic oxidation of 3,4-dihydroxymandelic acid with mushroom tyrosinase has been reported to yield 3,4-dihydroxybenzaldehyde via direct formation of a quinone methide intermediate²². Our data indicate the direct formation of an *o*-quinone as the major intermediate, but a quinone methide intermediate at minor levels may also be possible. The initial formation of the 3,4-dihydroxymandelic acid *o*-quinone has been proposed to occur in other electrochemical, chemical and enzymatic oxidations^{23,24}. The oxidative mechanism of the enzyme may or may not be the same as the oxidative mechanism involved electrochemically.

Two major chemical pathways have been proposed in the literature for the formation of 3,4-dihydroxybenzaldehyde from the 3,4-dihydroxymandelic acid through an initial *o*-quinone intermediate. One involves decarboxylation of the original *o*-quinone to an intermediate that forms 3,4-dihydroxybenzaldehyde, whereas in the second, the *o*-quinone reacts immediately with a molecule of substrate forming a charge-transfer complex, and through decarboxylation generates an intermediate which transforms into 3,4-dihydroxybenzaldehyde. The original *o*-quinone involved in the charge-transfer complex is then reduced back to 3,4-dihydroxymandelic acid^{25,26}. Our data suggest that this second mechanistic pathway is unlikely because this mechanism would produce a

reversible couple in the cyclic voltammogram of 3,4-dihydroxymandelic acid. This reversible couple would be due to the o -quinone of 3,4-dihydroxymandelic acid and the original substrate. The o -quinone would have to be stable at short time to be able to diffuse into bulk solution to form a charge-transfer-complex with starting substrate. Our data do not show a reversible couple to support this mechanism at times greater than approximately 0.5 seconds, therefore the quinone is not stable enough to form the charge-transfer-complex.

In conclusion, our data are consistent with a pathway in which the formation of 3,4-dihydroxybenzaldehyde by oxidation of 3,4-dihydroxymandelic acid occurs primarily through the generation of an o -quinone. This o -quinone then undergoes rate-determining unimolecular decarboxylation to form a quinone methide intermediate that subsequently rearranges to form 3,4-dihydroxybenzaldehyde (Fig. 12). Although a quinone methide is involved as a short-lived unobserved intermediate in this reaction mechanism, it is formed as a result of a homogeneous chemical reaction rather than by a heterogeneous electron transfer process.

Experimental Section

Solution Conditions

Electrochemical solutions (0.5 to 4.0 mM) of $2 \leq \text{pH} \leq 8$ were prepared by adjusting a 0.1 M potassium phosphate (KH_2PO_4) buffer solution with 0.1 M NaOH to the desired pH. Buffer solutions of $\text{pH} \leq 2$ were prepared with phosphoric acid and adjusted to the desired pH with 0.1 M NaOH. The solutions were purged with nitrogen for 5 minutes

before the start of experimentation. Chemicals were used as received from Aldrich or Sigma Chemical Companies.

Electrochemical Instrumentation

The cyclic voltammetric (CV) and chronoamperometric (SPSCA) experiments were performed using a three-electrode potentiostat which incorporated circuits for electronic correction of ohmic potential loss between the reference and working electrodes. This potential loss was normally small with the use of carbon paste electrodes in an aqueous solution. Control of the potentiostat, function generator and data acquisition for the SPSCA and CV data (for $v > 0.5 \text{ V s}^{-1}$) were performed with a laboratory digital computer (ADAC model 2000, LSI 11/2).

CV and the SPSCA experiments were conducted with a renewable carbon paste working electrode (0.5-cm diameter), a SCE reference electrode and a platinum flag auxiliary electrode. Coulometric experiments used a reticulated vitreous carbon working electrode that was separated from the SCE reference electrode and the platinum flag auxiliary electrode by a glass frit. The reticulated vitreous carbon (100 pores per linear inch) was purchased from The Electro Synthesis Co., Inc., East Amherst, N.Y. These coulometric electrodes were prepared by attaching a platinum wire via silver epoxy to a 2-in. x 2-in. x 1/2-in. block of vitreous carbon. Controlled-potential electrolysis was performed with a three-electrode potentiostat²⁷. All potentials are reported with respect to a SCE reference electrode.

Electrochemical Procedures

Cyclic voltammograms were taken in scan rate range from 0.2 to 50 V/s. After each cyclic voltammetric experiment the electrode surface

was renewed and the solution again purged with nitrogen. SPSCA was performed on the experimental CV solutions with the electrode surface being renewed before each run in order to minimize any adverse effects due to film formation. The initial potential was always set at 0.0 V for all compounds. The working potentials (Table 1) were varied depending on the experimental objective. During coulometric oxidations, solutions were purged with nitrogen. Aliquots were removed for HPLC analysis either at predetermined times and/or after two electrons per molecule of EAS had been removed.

HPLC and GC-MS Analysis of Oxidation Products

For LCEC (High Performance Liquid Chromatography with Electrochemical detection) analysis²⁸, electrochemical oxidation products were either directly injected or extracts (0.1 mL) of oxidative mixtures were adsorbed on alumina and the α -diphenols recovered in 1 M acetic acid prior to injection. The primary mobile phase consisted of methanol (10% v/v), and 0.1 M H_3PO_4 adjusted to pH 3.0 with NaOH. A second mobile phase consisted of methanol (11% v/v), 0.12 mM sodium octyl sulfate, 0.06 mM sodium EDTA and 0.1 M H_3PO_4 adjusted to pH 3.25 with NaOH. A C-18 column was employed with a flow rate of 1 mL/min. Products were detected with either a Kratos Analytical Spectraflow 757 absorbance detector set at 280 nm or a Bioanalytical Systems LC4B electrochemical detector operated at 720 mV. The identification of each oxidative metabolite was confirmed by comparing the retention time of the unknown peak with a known standard from the mandelic acid and benzaldehyde series using two different mobile phases. Co-injections of oxidation mixtures and known standards were also used to identify peaks.

Quantities of individual diphenols were calculated by comparing peak areas with that of an external standard.

GC-MS samples were lyophilized, resuspended in equal amounts of Rigisil and acetonitrile, and heated for 15 min. at 85 °C. Samples were then injected into a Hewlett-Packard 5790A GC containing a 30-m x 0.2-mm Supelco DB-1 bonded phase capillary column connected to a Hewlett-Packard 5970 mass-selective detector and a Hewlett-Packard 9133 data system. Retention times and mass spectra of reaction solutions were compared with authentic known samples of the chemicals. The GC-MS data were used to verifying the product identifications made by HPLC.

References:

- 1) Pryor, M.G.M.; Proc. R. Soc. B, 1940, 128, 393.
- 2) Sugumaran, M.; Molecular Entomology, 1987, 357-367.
- 3) Anderson, S.O.; A. Rev. Ent., 1979, 24, 29.
- 4) Anderson, S.O.; A. Rev. Ent., 1979, 24, 29.
- 5) Anderson, S.O.; Comprehensive Insect Physiol. Biochem. Pharmacol., 1985, 3, 59-74.
- 6) Brunet, P.C.J.; Insect Biochem., 1980, 10, 467.
- 7) Lipke, H.; Sugumaran, M.; Hanzel, W.; Adv. Insect Physiol., 1983, 17, 1.
- 8) Kramer, K.; Hopkins, T.; Arch. Insect Biochem. and Physiol., 1987, 6, 279-301.
- 9) Hopkins, T.; Kramer, K.; Physiology of Insect Epidermis. In Press, 1989.
- 10) Sugumaran, M.; Biochemistry, 1986, 25, 4489-4492.
- 11) Ortiz, F.M.; Serrano, J.T.; Lopez, J.N.R.; Castellanos, R.V.; Teruel, J.A.L.; Garcia-Canovas, F.; Biochim. Biophys. Acta, 1988, 957, 158-163.
- 12) Cabanes, J.; Sanchez-Ferrer, A.; Bru, R.; Garcia-Carmona, F.; Biochem. J., 1988, 256, 681-684.
- 13) Lipke, H.; Sugumaran, M.; Hanzel, W.; Adv. Insect Physiol., 1983, 17, 1.
- 14) Zeikus, J.G.; Adv. Microbiol. Ecol., 1981, 5, 211-243.
- 15) Larson, A.A.; Nature (London), 1969, 224-(5214), 25-27.
- 16) Papouchado, L.; Bacon, J.; Adams, R.N.; J. Electroanal. Chem. and Interfacial Electrochem., 1970, 24, App 1-5.
- 17) Ryan, M.; Yueh, A.; Wen-Yu Chen; J. Electrochem. Soc., 1980, 127, 1489-1495.
- 18) Hawley, M.D.; Adams, R.N.; J. Electroanal. Chem., 1964, 8, 1963-1966.

- 19) Ortiz, F.M.; Serrano, J.T.; Lopez, J.N.R.; Castellanos, R.V.; Teruel, J.A.L.; Garcia-Canovas, F.; *Biochim. Biophys. Acta*, **1988**, 957, 158-163.
- 20) Cabanes, J.; Sanchez-Ferrer, A.; Bru, R.; Garcia-Carmona, F.; *Biochem. J.*, **1988**, 256, 681-684.
- 21) Sugumaran, M.; *Biochemistry*, **1986**, 25, 4489-4492.
- 22) Sugumaran, M.; Lipke, H.; *Insect Biochem.*, **1983**, 13, No 3, 307-312.
- 23) Cabanes, J.; Sanchez-Ferrer, A.; Bru, R.; Garcia-Carmona, F.; *Biochem. J.*, **1988**, 256, 681-684.
- 24) Ortiz, F.M.; Serrano, J.T.; Lopez, J.N.R.; Castellanos, R.V.; Teruel, J.A.L.; Garcia-Canovas, F.; *Biochim. Biophys. Acta*, **1988**, 957, 158-163.
- 25) Cabanes, J.; Sanchez-Ferrer, A.; Bru, R.; Garcia-Carmona, F.; *Biochem. J.*, **1988**, 256, 681-684.
- 26) Ortiz, F.M.; Serrano, J.T.; Lopez, J.N.R.; Castellanos, R.V.; Teruel, J.A.L.; Garcia-Canovas, F.; *Biochim. Biophys. Acta*, **1988**, 957, 158-163.
- 27) Bartak, D.E.; Hundley, H.K.; Van Swaay, M.; Hawley, M.D.; *Chem. Instrum.*, **1972**, 4, 1-13.
- 28) Czapla, T.H.; Hopkins, T.L.; Kramer, K.J.; Morgan, T.D.; *Arch. Insect Biochem. and Physiol.*, **1988**, 7, 13-28.
- 29) Goulart, M.; Utley, J.; *J. Org. Chem.*, **1988**, 53, 2520-2525.
- 30) Proudfoot, G.; Ritchie, I.; *Aust. J. Chem.*, **1983**, 36, 885-894.
- 31) Chi-Sing Tse, D.; Kuwana, T.; *Anal. Chem.*, **1978**, 50, 1315-1318.
- 32) Kramer, K.; Nuntnarumit, C.; Aso, Y.; Hawley, M.D.; Hopkins, T.; *Insect Biochem.*, **1983**, 13, 475-479.
- 33) Saul, S.; Sugumaran, M.; *Febs Letters*, **1988**, 237, 155-158.

Table 1. Cyclic voltammetry and chronoamperometric data for the oxidation of catechol, substituted mandelic acids and benzaldehydes^a.

Compound	Cyclic Voltammetry		Chronoamperometry		Working Potential ^b (V)
	E _p (a) (V)	E _p (c) (V)	n	τ value	
Catechol	0.65	0.15	2		1.3
3,4-Dihydroxymandelic Acid	0.78	0.10, 0.01	2/4		1.2
3,4-Dihydroxybenzaldehyde	0.55	0.10, 0.01	2		1.1
3-Hydroxymandelic Acid	0.90		2		1.2
4-Hydroxymandelic Acid	0.95		2/0 F		1.2
3-Methoxy-4-Hydroxymandelic Acid	0.77		2/0 F		1.0
3-Hydroxy-4-Methoxymandelic Acid	0.80	0.15, 0.05	2/4		1.0
3-Methoxy-4-Hydroxybenzaldehyde	0.75		2/0 F		1.0

^a Cyclic voltammetry experiments were conducted at pH = 6.

^b Working potential for chronoamperometric experiments.

F Denotes fouling of the electrode surface occurred.

Table 2. Rate constants (k) for 3,4-dihydroxymandelic acid at several pH levels.

pH	k value (s ⁻¹)
1	0.20 ± 0.3
2	0.31 ± 0.2
4	0.84 ± 0.3
6	1.58 ± 0.2
7	2.45 ± 0.3
8	2.82 ± 0.4

Table 3. Analysis of coulometric oxidation products formed upon oxidation of methoxy derivatives of 3,4-dihydroxymandelic acid (1 mM) at different potentials after 2 e_a have been removed per molecule. Values are percent of original starting material oxidized.

Compound	Oxidation Potential (V)	3-Methoxy-4-Hydroxy-benzaldehyde %	3-Hydroxy-4-Methoxy-benzaldehyde %	3,4-Dihydroxy-benzaldehyde %	Remaining starting material %
3-Methoxy-4-Hydroxy-mandelic Acid ^b	0.8	14	-	0.2	43
	1.0 ^c	1	-	14	65
	1.0 ^d	2	-	2	56
	1.0 ^e	57	-	0.7	29
	1.2	2	-	2	68
3-Hydroxy-4-Methoxy-mandelic Acid ^b	0.6	-	4	4	45
	0.8	-	0.2	4	50
	1.2	-	0.2	19	63
3-Hydroxy-4-Methoxy-mandelic Acid ^f	1.2	1	-	25	57
	0.6	25	-	5	80
3-Methoxy-4-Hydroxy-mandelic Acid ^{f,g}					

^a Experimental error was within 5% of listed value. Values are the mean of 2 trials at each potential.

^b pH = 6.

^c New electrode.

^d Second oxidation experiment on new electrode.

^e Severely fouled electrode used.

^f pH = 2.

^g Analysis not conducted at pH 2 due to severity in which oxidation of this compound fouls the electrode surface.

Figure 1:

Proposed oxidative metabolites of N-acyl catecholamines involved in sclerotization of insect cuticle.

2 is formed during a Quinone Tanning mechanism.

3 is formed during Quinone Methide Sclerotization.

5 is formed during α,β -Sclerotization.

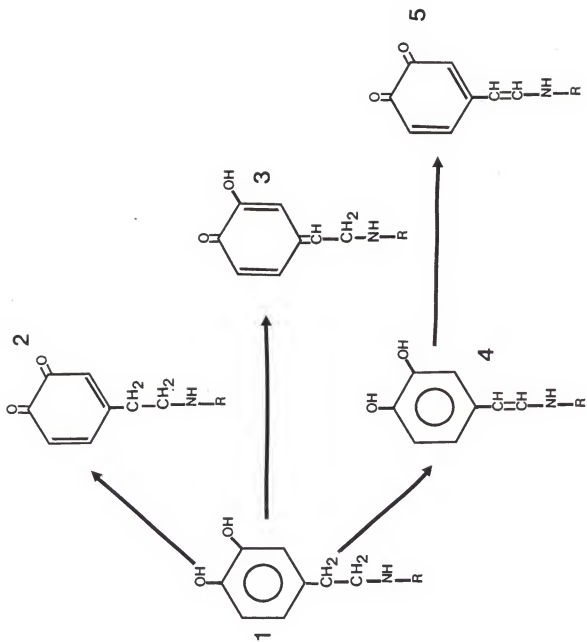


Figure 2:

Proposed cross-links between N-acyl catecholamines and proteins.

2 is from Quinone Tanning mechanism.

3 is from Quinone Methide Sclerotization.

5 is from α,β -Sclerotization.

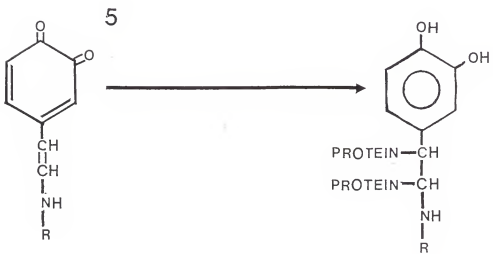
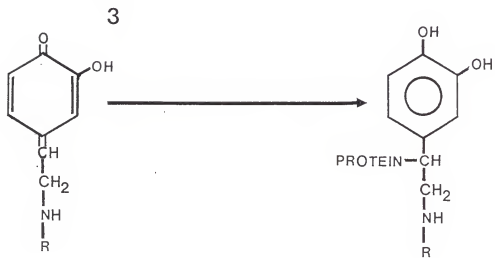
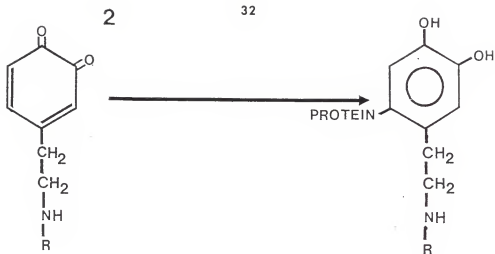


Figure 3:

Cyclic voltammogram for 1.45 mM 3,4-dihydroxymandelic acid at pH 2. The scan rate employed at a planar carbon paste working electrode (area = 0.78 cm²) was 0.2 V/s. The more positive cathodic peak increases in relative peak size with increasing scan rate while the second cathodic peak decreases in relative peak size with increasing scan rate. The first and second scans are denoted by a 1 and 2, respectively.

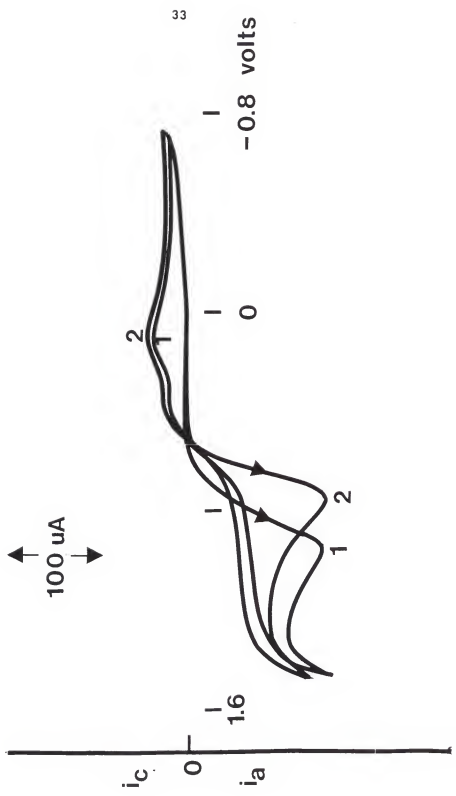


Figure 4:

Cyclic voltammogram for 2.04 mM 3,4-dihydroxybenzaldehyde at pH 2 with a scan rate of 0.066 V/s. A planar carbon paste working electrode with an area of 0.78 cm² was employed. The first and second scans are denoted by a 1 and 2, respectively.

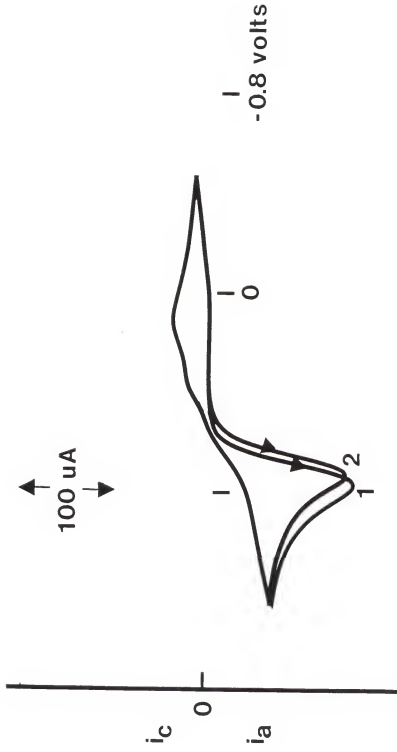


Figure 5:

Cyclic voltammogram for 2.04 mM 3,4-dihydroxybenzaldehyde at pH 2 with a scan rate of 0.2 V/s. A planar carbon paste working electrode with an area of 0.78 cm² was employed. The first and second scans are denoted by a 1 and 2, respectively.

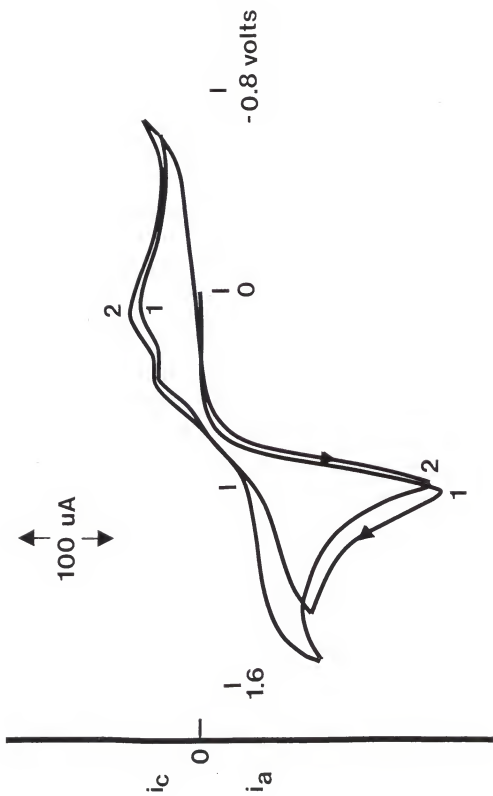


Figure 6:

Cyclic voltammogram for 2.04 mM 3,4-dihydroxybenzaldehyde at pH 2 with a scan rate of 0.66 V/s. A planar carbon paste working electrode with an area of 0.78 cm² was employed. The first and second scans are denoted by 1 and 2, respectively.

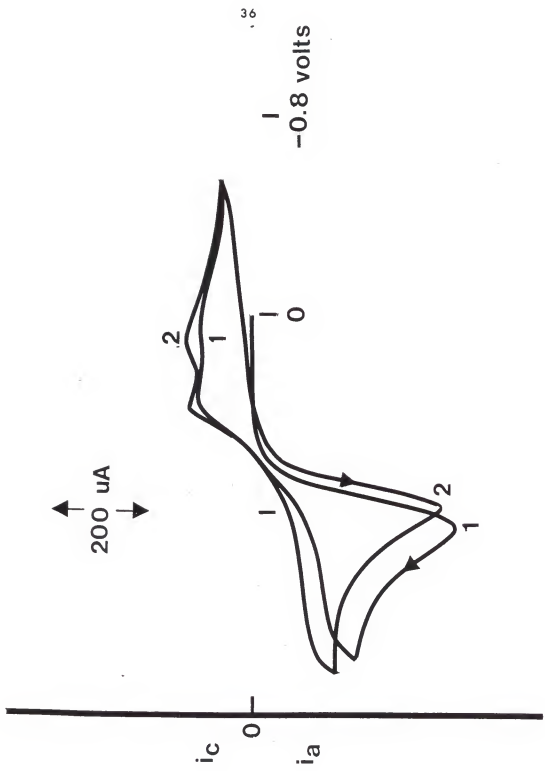


Figure 7:

Product levels after the controlled-potential oxidation of 3,4-dihydroxymandelic acid at pH 6 as a function of η value. Products were determined by UV absorbance at 280 nm after oxidation of a 1.08 mM solution and HPLC separation.

□ represents 3,4-dihydroxymandelic acid concentration

+ represents 3,4-dihydroxybenzaldehyde concentration.

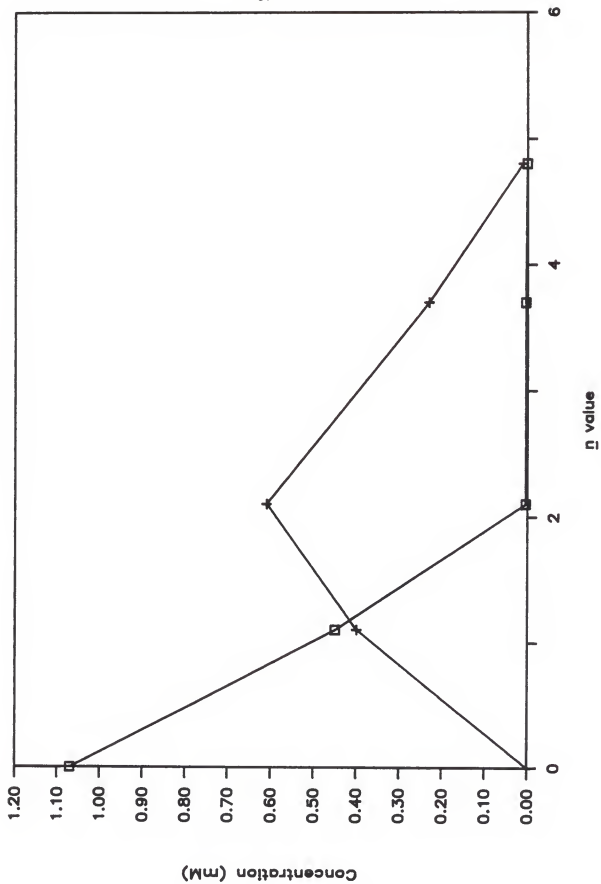


Figure 8:

Product levels after the controlled-potential oxidation of 3,4-dihydroxymandelic acid at pH 2 as a function of η value. Products were determined by UV absorbance at 280 nm after oxidation of a 0.94 mM solution and HPLC separation.

□ represents 3,4-dihydroxymandelic acid concentration

+ represents 3,4-dihydroxybenzaldehyde concentration.

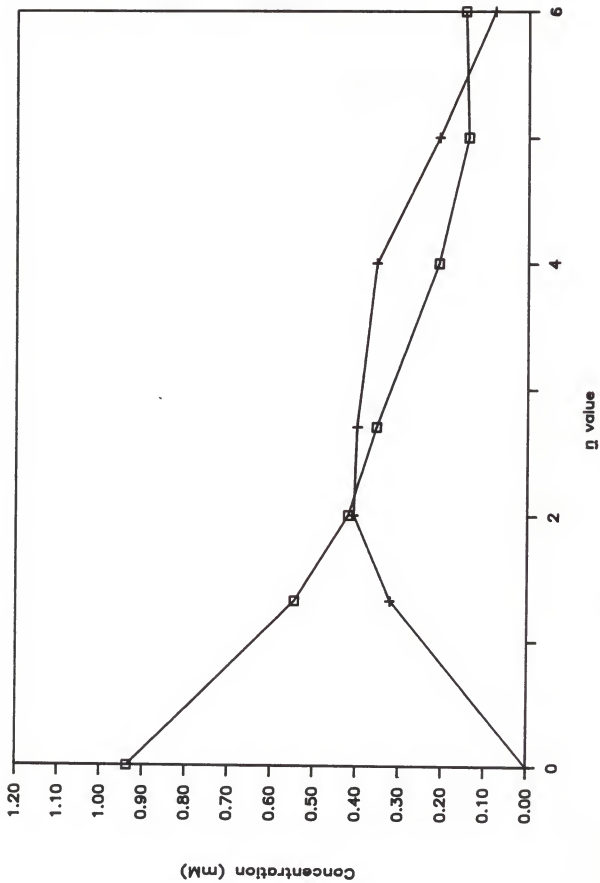


Figure 9:

Standard curves for various equilibrium values for an ECE mechanism in which a first-order chemical reaction is interposed between electron transfer processes. K is the value of the equilibrium constant for equation 4. Curves were obtained from digital simulations for an ECE reaction mechanism.

- represents $K = 0$
- + represents $K = 0.1$.
- ◇ represents $K = 0/0$.
- △ represents $K = 1.0$.
- X represents $K = 10$.
- ∇ represents $K = ∞$

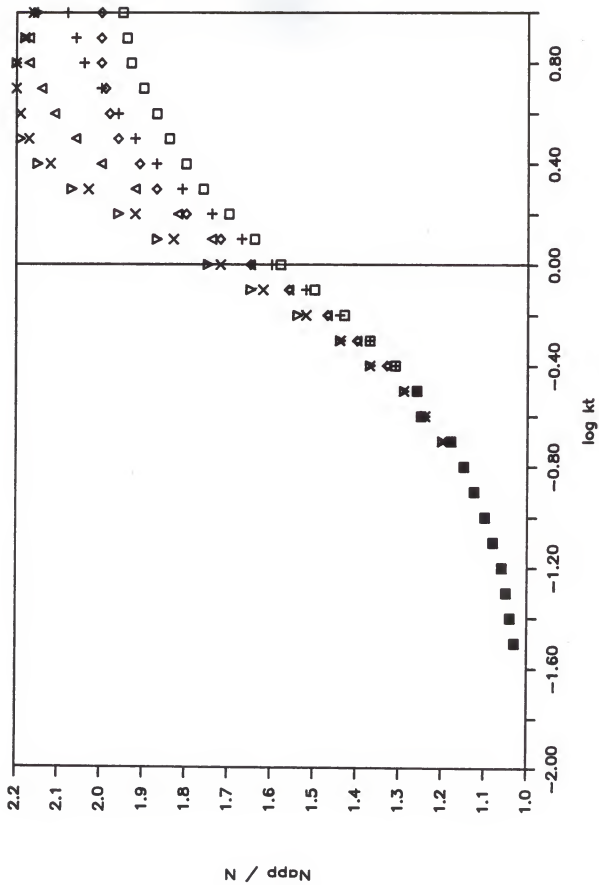


Figure 10:

Kinetic plot of SPSCA results for the oxidation of 3.40 mM 3,4-dihydroxymandelic acid at pH=6. The solid curve represents the theoretical curve for an ECE mechanism in which $k = 1.58 \text{ s}^{-1}$ and $K = 0/0$.

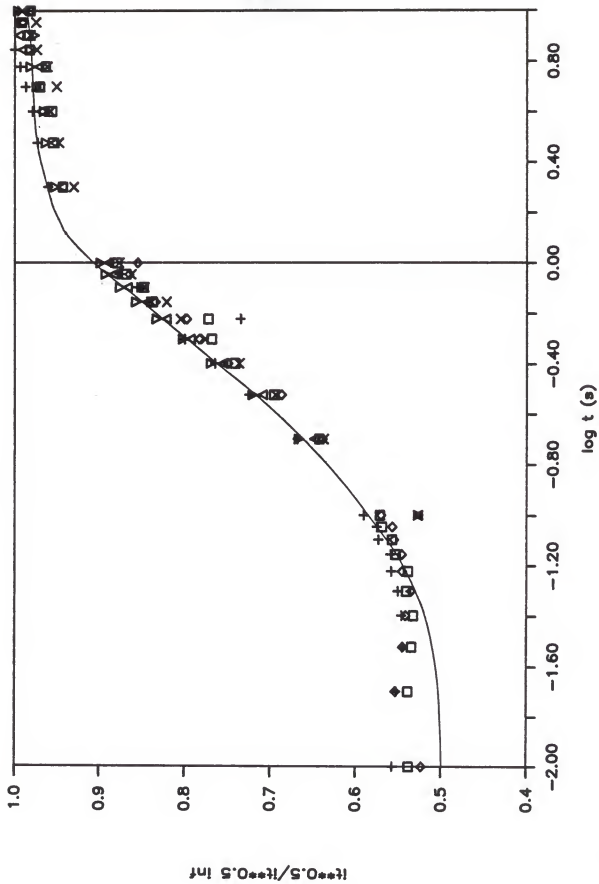


Figure 11:

Product levels after the controlled-potential oxidation of 4-hydroxymandelic acid at pH 6 as a function of n value. Products were determined by UV absorbance at 280 nm after HPLC separation.

□ represents 4-hydroxymandelic acid concentration

◇ represents 4-hydroxybenzaldehyde concentration

+ represents 3,4-dihydroxybenzaldehyde concentration

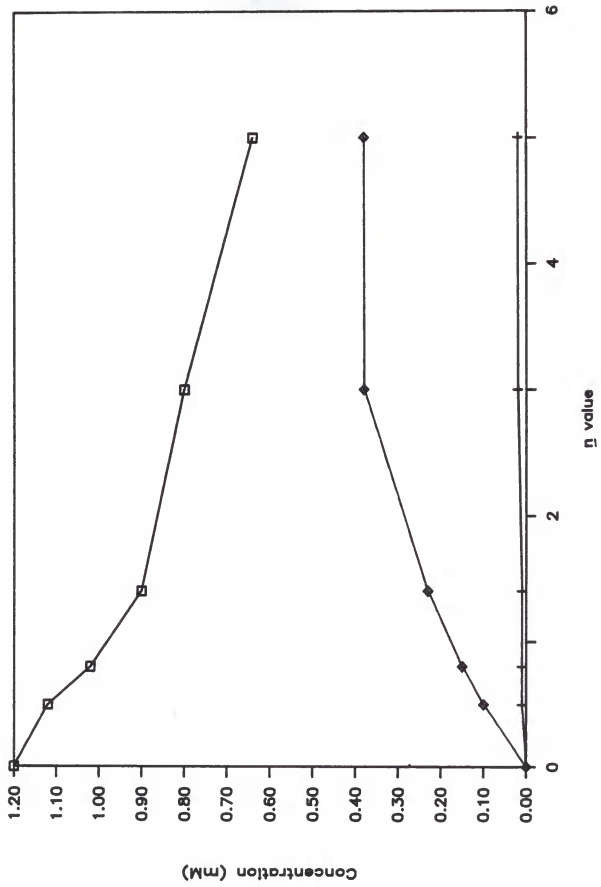
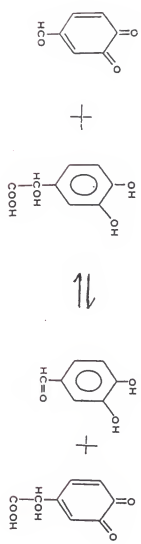
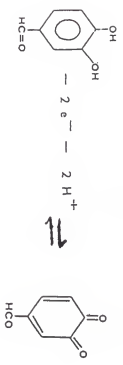
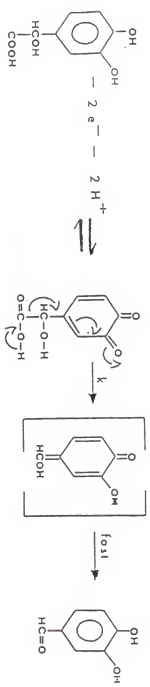


Figure 12:

Proposed Reaction Pathway for the Oxidative Decarboxylation
of 3,4-Dihydroxymandelic acid.



THE ELECTROCHEMICAL OXIDATION OF VARIOUS SUBSTITUTED MANDELIC
ACIDS: AN ELECTROCHEMICAL AND PRODUCT ANALYSIS STUDY

by

MAURICE ROGER CLAEYS

B.A., Coe College, 1987

AN ABSTRACT OF A THESIS

submitted in partial fulfillment of the

requirements for the degree

MASTER OF SCIENCE

CHEMISTRY

KANSAS STATE UNIVERSITY

Manhattan, Kansas

1989

ABSTRACT

Oxidative mechanistic pathways of 3,4-dihydroxymandelic acid and related compounds were studied by cyclic voltammetry, single-potential-step chronoamperometry, and controlled-potential coulometry. Results show 3,4-dihydroxymandelic acid electrochemically oxidizes by an ECE mechanism forming 3,4-dihydroxybenzaldehyde. Evidence was obtained that supports the formation of an initial *o*-quinone intermediate, which subsequently undergoes rate-determining decarboxylation to give a transient *p*-quinone methide. This latter, unobserved species undergoes rapid rearrangement to form 3,4-dihydroxybenzaldehyde. The rate constant for the decarboxylation was found to be $k = 1.58 \text{ s}^{-1}$ at pH=6 and varied monotonically from pH 1 to pH 8. Evidence for this mechanistic pathway is supported by the electrochemical oxidation of various methoxy analogs of 3,4-dihydroxymandelic acid.

Important terms:

electrochemical; 3,4-dihydroxymandelic acid; *o*-quinone; quinone methide; 3,4-dihydroxybenzaldehyde; oxidation.